A Wavelet-Based Activation Detector for Bipolar Electrogram Analysis During Atrial Fibrillation

Alejandro Alcaine[1,2], Fernando Simón[1,2], Ángel Arenal [3], Pablo Laguna[1,2], Juan Pablo Martínez[1,2]

[1]Communication Technologies Group (GTC), Aragón Institute of Engineering Research (I3A), IIS Aragón, Universidad de Zaragoza, Zaragoza, Spain
[2]Biomedical Research Networking Center in Bioengineering, Biomaterials and Nanomedicine (CIBER-BBN), Zaragoza, Spain
[3]Department of Cardiology, Gregorio Marañón General University Hospital, Madrid, Spain

Abstract

It has been shown that computation of atrial fibrillation (AF) electrogram (EGM) indices based on activation times is limited by the accuracy of the activation detector. In this work, a wavelet-based detector is proposed as a method to reliably extract activation time locations from the wavelet decomposition of non-linearly pre-processed bipolar EGM signal. A more classical amplitude adaptive threshold-based detector was also implemented for comparison purposes. Evaluation and validation was made by means of two scenarios due to the lack of standard databases: First, a simulation study where four real EGM signals, selected for its high SNR, were contaminated with noise at different SNR levels and detection performance was evaluated. Second, the inverse of the median activation cycle length (ACL) obtained from both detectors was compared with the spectral dominant frequency considered as gold standard. The proposed detector is more accurate and reliable than the threshold-based approach in the presence of noise, allowing a more reliable computation of activation-time-based AF clinical indices.

1. Introduction

Atrial fibrillation is one of the most common arrhythmias whose prevalence increases with population aging [1]. AF is characterized by a very rapid, chaotic and desynchronized electrical activity of the atria followed by irregular ventricular response. As a result, there is an inefficient contraction of the atrium which may be cause of heart stroke, cerebrovascular accident and/or congestive heart failure.

The mechanisms sustaining AF are continuously investigated, involving rapid foci and/or reentry circuits with rotors and multiple wavelets [2,3]. Thus, EGM signals are characterized by very non-stationary, irregular and noisy signals as shown in Figure1.a).

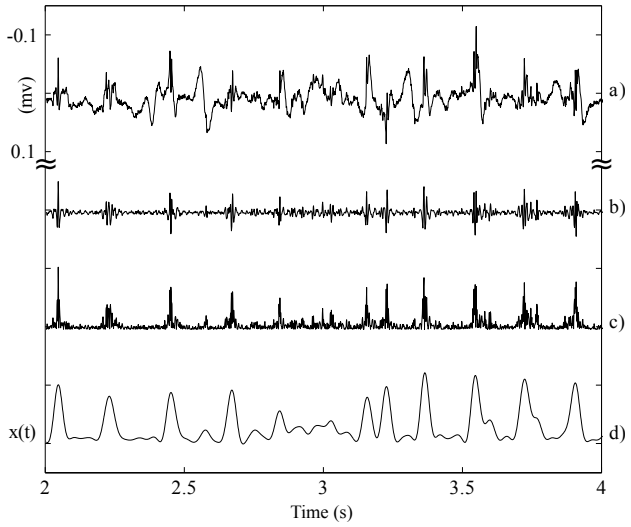

Figure 1. EGM pre-processing filtering steps: a) Original EGM signal, b) band-pass filtered signal, c) rectified version of b), and d) low-pass filtered signal.

A recent simulation study showed that time-based measurement of EGM organization and synchronization were more affected by noise than frequency-based or cross-correlation-based indices [4]. This can be explained by the lack of robustness against noise of the activation detector used for deriving those indices.

Activation detection is a challenging task due to the morphology variability of EGM signals during AF. Several approaches have been previously proposed, Barbaro and coworkers proposed an amplitude thresholding detection [5] and based on this idea, an adaptive thresholding approach was proposed in [6]. Other approaches have been proposed for atrial activation location using the non-linear energy operator [7] or the continuous wavelet transform for

activation cycle length measurements [8] and for location and analysis of fractionated unipolar EGM signals combined with template matching techniques and rules [9].

In this work, we propose and evaluate an automatic algorithm based on the wavelet transform for reliable location of activation times on bipolar EGMs.

2. Materials

Recordings used for this study belong to 20 patients admitted for ablation procedure during AF at Hospital Gregorio Marañón, Madrid (Spain), registered using a 20-pole circular *Lasso®* catheter (*Biosense Webster Inc.*) placed in pulmonary veins with 977 Hz sampling frequency.

3. Methods

3.1. EGM pre-processing

A non-linear filtering technique based on [10] was applied to the signal, i.e., band-pass filtering using a fourth order Butterworth filter with 40 and 250 Hz cut-off frequencies, then output rectification and finally a low-pass filtering using a fourth order Butterworth filter with 20 Hz cut-off frequency. This pre-processing allows to simplify the signal removing baseline and high frequency components and enhance the high energy components which are more feasible to belong to an atrial activation. These filtering steps are shown in Figure 1.

3.2. Frequency indices

For every ten-second segment of EGM the power spectral density (PSD) was estimated by means of Welch's method with a two-second length Hamming window and 50% overlapping. Then, the dominant frequency (DF) ,f_D, was defined as the maximum spectral peak within 1.5 to 20 Hz.

From the estimated PSD, we also measured the regularity index (RI), defined as the percentage of the total power area lying within $f_D \pm 0.75$ Hz and organization index (OI), defined as the percentage of total power area around f_D and its harmonics.

3.3. Wavelet transform

The wavelet transform (WT) is a decomposition of the signal as a combination of a set of basis function obtained by dilation a and translation b of a single prototype wavelet $\psi(t)$. Thus the WT of a signal $x(t)$ is defined as

$$W_a x(b) = \frac{1}{\sqrt{a}} \int_{-\infty}^{+\infty} x(t) \psi \left(\frac{t-b}{a} \right) dt, a > 0, \quad (1)$$

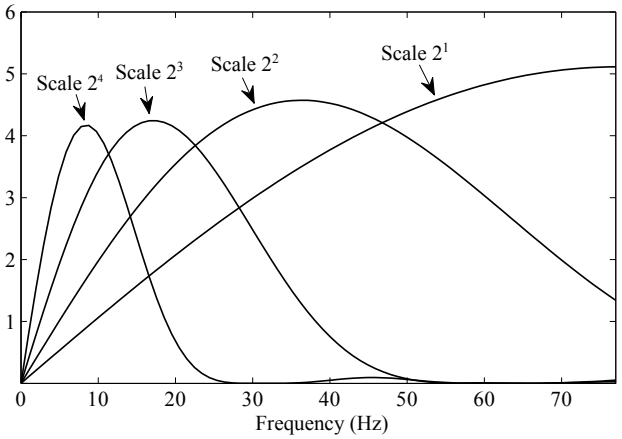

Figure 2. Equivalent transfer functions of the discrete wavelet transform at scales 2^k , $k = 1 \cdots 4$ for an interpolation sampling frequency of 1000 Hz.

where scale parameter a modify the bandwidth and time resolution at each scale. If the prototype wavelet $\psi(t)$ is the derivative of a smoothing function $\theta(t)$, the WT of a given signal $x(t)$ at scale a can be written as

$$W_a x(b) = -a \left(\frac{d}{db} \right) \int_{-\infty}^{+\infty} x(t) \theta_a(t-b) dt, \quad (2)$$

where $\theta_a(t) = (1/\sqrt{a})\theta(t/a)$ is the scaled version of the smoothing function. Therefore the WT at scale a is proportional to the derivative of the filtered version of the signal with a smoothing impulse response at the current scale a. Thus the zero-crossings of the WT correspond to the local maxima or minima of the smoothed signal at different scales, and maximum values of the WT are associated with maximum slopes in the smoothed signal. In our application, we are interested in detecting atrial activations which are composed of local maxima at different scales occurring at different times because of AF activation wavefronts.

To implement the WT, time and scale were discretize following the *dyadic discrete wavelet transform* (DWT) using the *algorithme à trous* [11] which allows to keep the time resolution of the signal representation by removing the decimation stages and interpolating the filter impulse response of the previous scale in Mallat's algorithm [12].

We used the derivative of a quadratic spline, used and validated for ECG delineation in [13, 14], as prototype wavelet, $\psi(t)$, which Fourier transform has the form

$$\Psi(\Omega) = j\Omega \left(\frac{sin(\frac{\Omega}{4})}{\frac{\Omega}{4}} \right)^4, \quad (3)$$

thus, the wavelet can be interpreted as the derivative of the convolution of four rectangular pulses, i.e., the derivative of a low-pass function. According to Mallat's algorithm

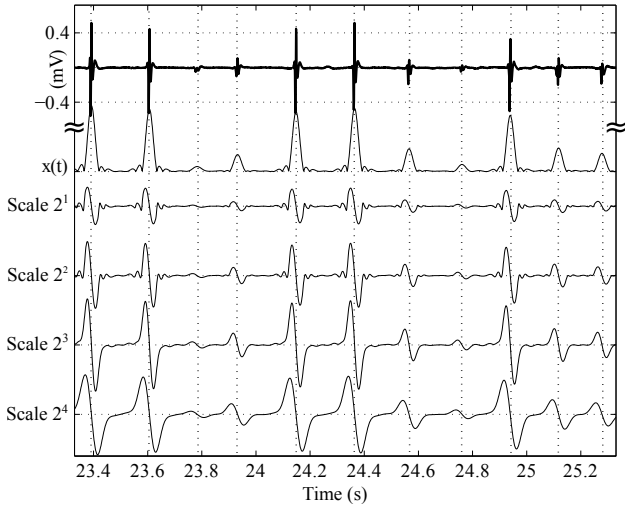

Figure 3. WT at the first four scales of a real pre-processed EGM signal $x(t)$.

and using the *algorithme à trous*, the transfer functions of the first four scales interpolated at 1000 Hz sampling frequency are presented in Figure 2 showing that this filter behaves as low-pass filter differentiators.

3.4. Detection algorithm

The pre-processed EGM signal has most of its energy component within 0 to 20 Hz. According to the wavelet transfer functions detailed in Figure 2, atrial activation frequency components lie at scales 2^3 and 2^4.

Figure 3 shows the WT of a preprocessed EGM signal where the more energetic activations are at scales 2^3 and 2^4. Based on the properties of the WT, activations were detected using the multi-scale approach proposed by Li *et al.* [13], this algorithm searches across scales for *"maximum modulus lines"* which exceed a threshold at every considered scale. The threshold is defined for this application by means of the root mean square (RMS) value of the considered scale. Thus, after removing all isolated and redundant maximum lines, the zero-crossings at scale 2^1 between two successive lines exceeding the threshold at scale 2^4 are marked as atrial activations.

Other protections were taken, as a blanking period of 95 ms where any new activation detection before this blanking period were deleted and considered with no physiological meaning [15]. In addition a back search with five threshold reduction steps at scale 2^3, which is as energetic as scale 2^4 but noisier due to its wider bandwidth, was included.

4. Results

Due to the lack of standard databases with activation annotated by expert physicians, detectors performance was estimated in two scenarios:

Simulation: Four selected two-minute length real EGM based on their high signal-to-noise ratio (SNR) were used as *"clean signals"*, then were contaminated with 200 realizations of additive Gaussian white noise (AWGN) at different SNR levels from 15 dB to -5 dB in increments of 5 dB. To assess the detector performance, we computed sensitivity, $Se = TP/(TP + FN)$, and positive predictive value, $P^{+} = TP/(TP + FP)$, where TP stands for the number of true detections, FN stands for the number of miss detections and FP stands for the number of false detections. Those indices were measured referred to a manually annotated activations set in the clean signals.

In order to compare performance of both detectors, F_1-score was also computed as

$$F_1\text{-score} = \frac{2TP}{2TP + FP + FN}, \tag{4}$$

which can be interpreted as the harmonic mean between Se and P^{+}. Table 1 shows mean $\pm$ standard deviation (SD) of Se, P^{+} and F_1-score for all considered recordings and SNR level where can be seen that the wavelet-based approach outperforms the threshold-based approach at all SNR levels.

Clinical indices: From the 20 records (10 EGM each), those signals with low quality and/or RI < 0.2 were rejected resulting in 169 total signals to study. Spectral DF of every signal was compared with the median of the inverse ACL from both detectors. The error of deriving DF as the inverse of the ACL is -0.2 ± 0.4 Hz with the wavelet-based approach, in contrast with 0.6 ± 1.2 Hz for the threshold-based approach.

5. Discussion and conclusions

Location of time-based activations measured on intra-atrial signals during AF is a challenging task due to the noise and morphology variability of EGM signals.

A wavelet-based atrial activation detector is proposed due to the lack of robustness of classical detectors against noise and unorganized EGM signals which culminates in a poor performance of derived time-based indices for AF characterization.

In the first scenario we compared and evaluate both approaches using four high SNR selected EGM recordings which were contaminated with AWGN at different SNR levels. In this scenario, high Se and P^{+} values were reached with both detectors. Table 1 shows that the threshold-based approach yields in higher Se values than the wavelet-based approach, but its P^{+} values decrease faster with low SNRs. F_1-score takes into account of both Se and P^{+} behavior and shows that for every SNR level, the wavelet-based approach outperforms the

Table 1. Detectors performance.

	Wavelet-based approach			Threshold-based approach		
SNR (dB)	Se (%)	P^+ (%)	F_1-score (%)	Se (%)	P^+ (%)	F_1-score (%)
15	96.1 ± 4.8	99.3 ± 0.8	97.7 ± 2.9	93.1 ± 7.8	99.6 ± 0.5	96.1 ± 4.3
10	94.3 ± 6.7	98.0 ± 2.3	96.0 ± 4.8	94.3 ± 7.4	93.4 ± 7.7	93.9 ± 7.5
5	91.0 ± 9.0	95.0 ± 4.9	92.9 ± 7.0	93.7 ± 7.5	78.8 ± 12.8	85.4 ± 10.8
0	87.3 ± 9.8	88.3 ± 9.9	87.7 ± 10.0	91.7 ± 7.1	68.4 ± 13.7	78.0 ± 11.7
-5	78.5 ± 10.2	76.7 ± 13.4	77.3 ± 11.9	86.7 ± 7.6	50.9 ± 10.3	63.9 ± 10.2

threshold-based approach and its decreasing performance with high noise levels is less steep.

In the second scenario, classic DF was compared with the inverse of the median ACL obtained from both detectors showing that the wavelet-based approach result in smaller error in DF estimation than the threshold-based approach.

This work shows that the proposed wavelet-based approach is more accurate in comparison with the threshold-based approach. The results of second scenario shows that the detections made with the proposed method could be a good alternative for measuring time-based indices of AF characterization like the inverse of the median ACL, which can be a good surrogate of classical DF computation. Furthermore, the lack of standard databases with audited annotations makes performance comparison difficult. Testing databases with more signals and computation of different time-based AF characterization indices should be introduced in future works.

Acknowledgements

This study was partially supported by a FPI grant to AA ref: BES-2011-046644, by project TEC2010-21703-C03-02 from Ministerio de Economía y Competitividad, Gobierno de España, and by DGA through Grupo Consolidado GTC. The CIBER-BBN is an initiative of Instituto de Salud Carlos III.

References

[1] Miyasaka Y, Barnes ME, Gersh BJ, Cha SS, Bailey KR, Abhayaratna WP, Seward JB, Tsang TS. Secular trends in incidence of atrial fibrillation in olmsted county, minnesota, 1980 to 2000, and implications on the projections for future prevalence. Circulation 2006;114(2):119–25.

[2] Nattel S. New ideas about atrial fibrillation 50 years on. Nature 2002;415(6868):219–26.

[3] Schotten U, Verheule S, Kirchhof P, Goette A. Pathophysiological mechanisms of atrial fibrillation: A translational appraisal. Physiological Reviews 2011;91(1):265–325.

[4] Simon F, Arenal A, Laguna P, Martinez JP. Comparison of electrogram organization and synchronization indices in atrial fibrillation: A simulation study. In Proc. Computing in Cardiology. 2011; 181–84.

[5] Barbaro V, Bartolini P, Calcagnini G, Censi F, Michelucci A. Measure of synchronisation of right atrial depolarisation wavefronts during atrial fibrillation. Medical and Biological Engineering and Computing 2002;40:56–62.

[6] Richter U, Bollmann A, Husser D, Stridh M. Right atrial organization and wavefront analysis in atrial fibrillation. Medical and Biological Engineering and Computing 2009; 47(12):1237–46.

[7] Schilling C, Nguyen MP, Luik A, Schmitt C, Dössel O. Non-linear energy operator for the analysis of intracardial electrograms. In IFMBE World Congress on Medical Physics and Biomedical Engineering, Munich, Germany, volume 25 (4). 2009; 872–75.

[8] Dubois R, Roussel P, Hocini M, Sacher F, Haissaguerre M, Dreyfus G. A wavelet transform for atrial fibrillation cycle length measurements. In Proc. Computing in Cardiology. 2009; 501–4.

[9] Houben R, de Groot N, Allessie M. Analysis of fractionated atrial fibrillation electrograms by wavelet decomposition. IEEE Trans Biomed Eng 2010;57(6):1388–98.

[10] Botteron G, Smith J. A technique for measurement of the extent of spatial organization of atrial activation during atrial fibrillation in the intact human heart. IEEE Trans Biomed Eng 1995;42(6):579–86.

[11] Cohen A, Kovačević J. Wavelets: The mathematical background. In Proc. IEEE, volume 84. 1996; 514–22.

[12] Mallat S, Zhong S. Characterization of signals from multiscale edge. IEEE Trans Pattern Anal Machine Intell 1992; 14:710–32.

[13] Li C, Zheng C, Tai C. Detection of ecg characteristic points using wavelet transforms. IEEE Trans Biomed Eng 1995; 42(1):21–28.

[14] Martinez JP, Almeida R, Olmos S, Rocha AP, Laguna P. A wavelet-based ecg delineator: evaluation on standard databases. IEEE Trans Biomed Eng 2004;51(4):570–81.

[15] Slocum J, Sahakian A, Swiryn S. Diagnosis of atrial fibrillation from surface electrocardiograms based on computer-detected atrial activity. Journal of Electrocardiology 1992; 25(1):1–8.

Address for correspondence:

Alejandro Alcaine Otín
C/ Mariano Esquillor S/N, Edificio I+D+i, L 4.0.05
50018 Zaragoza, Spain.
E-mail: aalcaineo@unizar.es